Journal of the Meteorological Society of Japan, Vol. 75, No. 1, pp. 1–11, 1997

Instability of a Front with a Layer of Uniform Potential Vorticity

By Keita Iga

Ocean Research Institute, University of Tokyo, Tokyo 164, Japan

(Manuscript received 25 May 1995, in revised form 1 October 1996)

Abstract

The linear stability of a front whose lower layer has a uniform potential vorticity is investigated. The results are compared with the unstable modes of a frontal model which consists of two homogeneous flows with an interacting interface. Unstable modes with a phase speed close to the velocity of the basic flow in the lower layer, which exist in the frontal model of two homogeneous flows, are stabilized in the present model. This feature is explained by the absence of Rossby waves in the reduced one-layer problem of the lower layer resulting from the uniformity of its potential vorticity. The results show that the stability of a front is strongly affected by the potential vorticity distribution. Careful attention is needed for the application of the frontal model with uniform potential vorticity, which is a critical situation.

1. Introduction

The linear instability of a front which consists of two homogeneous flows provides a theoretical basis for understanding the atmospheric disturbances associated with frontal systems. It was originally formulated by Kotschin (1932) and the unstable modes that develop upon it were obtained by Orlanski (1968). The same problem was recently reconsidered and explained in physical terms by Iga (1993). The analysis of such a simple model should be useful in understanding the basic characteristics of frontal instability as it exists in the atmosphere. However, it is apparent that any real situation has characteristics that are different from those of the model.

Figure 1 shows a convergent cloud band over the western part of the Japan Sea in winter as simulated in a forecasting model. This band has a frontal structure (Fig. 2) like other cases (*e.g.*, Nagata, 1987), where a disturbance develops later to become a meso-scale low. This frontal surface is not a plane like the model formulated by Kotschin (1932) shown in Fig. 3a, but its inclination becomes steeper as it approaches the ground. Moreover, the velocity in a layer, in particular in the lower layer, is not constant but varies depending on the distance from the surface front. In the lower layer, it is not the velocity but potential vorticity which is almost uniform as shown in Fig. 2. Considering the formation process of this front, it is more natural for the lower layer to have homogeneous potential vorticity, rather than to have a homogeneous velocity distribution, since the origin of the air in the lower layer is a large-scale cold airmass formed over the continent. However, when applying a theory to this phenomenon, the results of the analysis of the frontal model with two uniform-flow layers, whose basic state is very easy to describe, were often used (*e.g.*, Yamaguchi and Magono 1974). Here arises a question: how far can we apply the results of the analysis of the model formulated by Kotschin (1932) to such a situation? Can we derive qualitatively the same conclusion, or does the situation of almost constant potential vorticity lead to substantial differences? If there is no essential difference, it may be appropriate to apply the theory of the frontal model which consists of two uniform flows to such fronts over the Japan Sea, but, if the uniformity of the potential vorticity has a crucial influence on its stability, we must reconsider carefully the structure of such fronts. In this paper, we will consider frontal waves at a front whose lower layer has uniform potential vorticity (Fig. 3b), and investigate how far we can apply the qualitative features of simplified models like that of Kotchin (1932).

The frontal model treated in this paper itself is still quite a simplified one. Recently, analysis of the stability of fronts with continuous stratification has been attempted (*e.g.*, Snyder, 1995; Moore and Peltier, 1990). One could in principle analyze complicated models with various effects in order to investigate detailed features of each situation. However, we want to focus here on qualitative discussions: how far we can apply results of a certain simple model to other situations, or what conditions al-

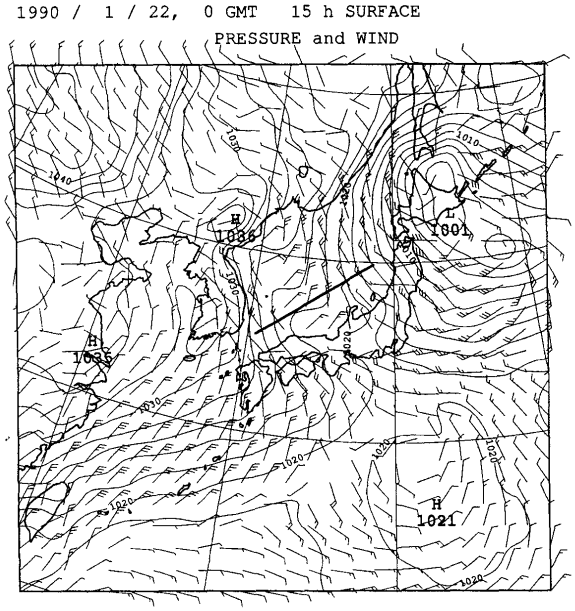

Fig. 1. Sea-level pressure and lowermost-level wind predicted by the Japan Spectral Model (JSM), after 15 hours using the initial data at 00 Z, January 22, 1990. A convergence zone is formed over the western part of the Japan Sea.

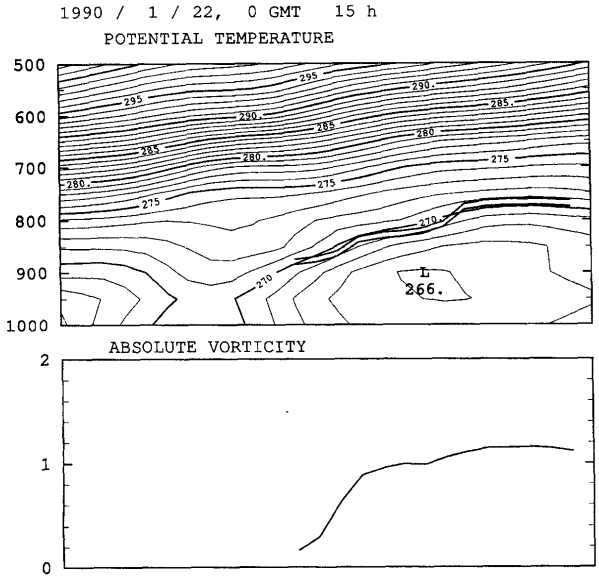

Fig. 2. Cross section (potential temperature) and absolute vorticity in the lower layer along the thick line in Fig. 1. The value of absolute vorticity ($f - dU/dy$) is normalized by f. A double thick line indicates the frontal surface defined as level where the vertical gradient of potential temperature is maximal. Proportionality between the height of frontal surface and the absolute vorticity in the lower layer shows the uniformity of the potential vorticity in the lower layer.

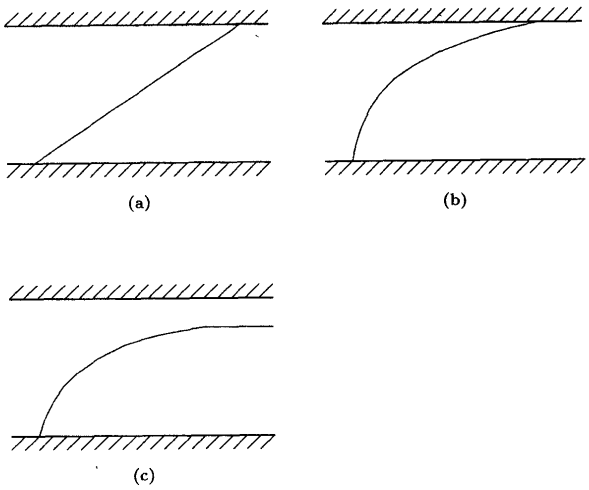

Fig. 3. (a) Frontal model investigated by Kotschin (1932), Orlanski (1968) and Iga (1993). (b) Frontal model investigated in this paper. (c) Frontal model investigated by Killworth *et al.* (1984).

ter, in a fundamental manner, the stability of fronts. Although analysis of frontal models with continuous stratification have been made, there are still many restrictions; Snyder (1995), for example, obtained the unstable modes indirectly by time integration. Moore and Peltier's (1990) work does not suffer from this problem. However, there are questions as to the role that the boundary conditions employed had on the results obtained. Analysis of a simpler model will be more appropriate to reveal qualitative conclusions. For example, it allows one to identify the origins of each mode of instability. Therefore, we choose to analyze a simpler model in this paper. The computations were done at sufficiently high resolution so as to resolve the qualitative features of the simulation (see Appendix).

There are other studies of a frontal model with a layer of uniform potential vorticity, in particular as a model of fronts in the ocean. In most models of this sort such as Paldor (1983 a,b) and Kubokawa (1986), the lower layer has an infinite depth, so that the situation is essentially a one-layer problem. On the other hand, a two-layer model with the configuration shown in Fig. 3c was investigated by Killworth *et al.* (1984). In all these studies, the frontal interface does not intersect the sea bottom.

Comparing the model formulated by Kotschin (1932) with that treated by Killworth *et al.* (1984), we notice two important differences; the uniformity of the potential vorticity and the configuration whether the frontal surface intersects both (upper and lower) boundaries. Thus, we cannot directly conclude which of the differences is responsible for the differences between the results of Iga (1993) and those of Killworth *et al.* (1984). The model inves-

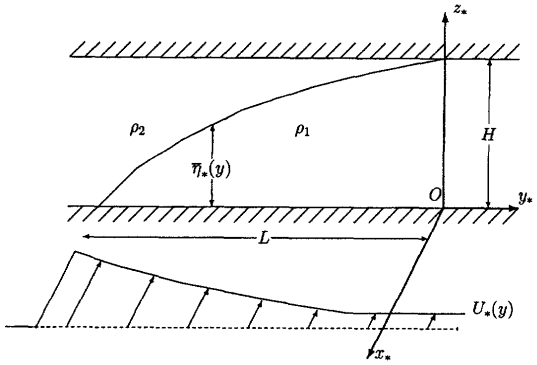

Fig. 4. Frontal surface model The lower layer has a uniform potential vorticity.

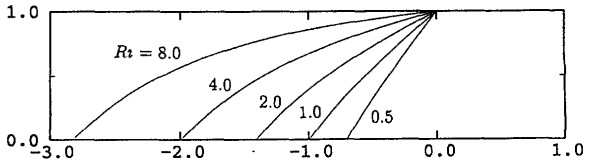

Fig. 5. Configuration of the frontal surface for various values of Ri. The unit of horizontal scale is λ_R.

tigated in this paper fills this gap; it differs from the model of Kotschin (1932) by the uniformity of the potential vorticity, and from that of Killworth *et al.* (1984) by having an interface intersecting both boundaries. Hence, by investigating this model, we will be able to identify how the two conditions affect the unstable modes.

First, we will derive basic equations in Section 2. In Section 3, the numerical solutions are shown. We will describe one-layer problems which are necessary to interpret the unstable modes in the two-layer problem in Section 4, and classify the unstable modes obtained. We will compare the results obtained with those of Iga (1993) in Section 5.

2. Basic equations

2.1 Basic sate

We consider a front which consists of two layers of incompressible homogeneous fluid bounded above and below by rigid horizontal planes at $z_* = 0$ and $z_* = H$. We assume that the fluid of the lower layer has a uniform potential vorticity and that upper layer has a uniform velocity. We can assume the fluid in the upper layer is at rest by considering a coordinate system moving with the velocity of the upper layer (Fig. 4).

The basic equations for this problem are the same as (1), (2) and (3) in Iga (1993). First, we will describe the basic state. The equations for geostrophic balance, hydrostatic balance and uniform potential vorticity of the first (lower) layer are

$$0 = -fU_* - \frac{1}{\rho}\frac{dP_{*1}}{dy_*}, \tag{2.1}$$

$$P_{*1} - P_{*2} = \Delta\rho g\overline{\eta}_*, \tag{2.2}$$

$$\frac{f - \dfrac{dU_*}{dy_*}}{\overline{\eta}_*} = \frac{f}{H}. \tag{2.3}$$

If we assume that the fluid in the upper layer is at rest, we can assume without loss of generality $P_{*2} \equiv 0$. Then, from (2.1) and (2.2), we obtain

$$U_* = -\frac{\Delta\rho g}{\rho f}\frac{d\overline{\eta}_*}{dy_*}, \tag{2.4}$$

and from (2.3)

$$\overline{\eta}_* = H\left(1 - \frac{1}{f}\frac{dU_*}{dy_*}\right). \tag{2.5}$$

Substituting (2.5) into (2.4), we obtain a differential equation with respect to U_*

$$U_* = \frac{\Delta\rho g H}{\rho f^2}\frac{d^2U_*}{dy_*{}^2}. \tag{2.6}$$

Under the boundary condition of $dU_*/dy_* = 0$ at $y_* = 0$, this yields

$$U_* = -Cf\lambda_R \cosh\left(\frac{y_*}{\lambda_R}\right), \tag{2.7}$$

$$\overline{\eta}_* = H\left(1 + C\sinh\left(\frac{y_*}{\lambda_R}\right)\right), \tag{2.8}$$

$$\text{where} \quad \lambda_R \equiv \frac{1}{f}\left(\frac{\Delta\rho g H}{\rho}\right)^{1/2},$$

where C is the constant of integration and the only non-dimensional parameter which characterizes the basic state. However, in this paper as in Orlanski (1968) and Iga (1993), we will use Ri defined as square of the ratio of the frontal-zone width L to the Rossby's radius of deformation λ_R instead of C as the non-dimensional parameter characterizing the basic state. The width L satisfies

$$\begin{aligned}\overline{\eta}_*(-L) &= \overline{\eta}_*(-Ri^{1/2}\lambda_R)\\ &= H\left(1 - C\sinh Ri^{1/2}\right)\\ &= 0,\end{aligned}$$

and thus, the parameter C is expressed by Ri as

$$C = 1/\sinh Ri^{1/2}. \tag{2.9}$$

Shapes of the frontal surface for various values of Ri are shown in Fig. 5. If Ri is small enough, the frontal surface becomes more plane and the velocity distribution is indistinguishable from that of the frontal model which consists of two homogeneous flows.

2.2 Equations for disturbance and boundary conditions

We consider the perturbed motion on this basic state. The variables are partitioned into the basic part and the disturbance part as follows:

$$u_{*1} = U_* + u'_{*1}\ ,\ u_{*2} = u'_{*2}\ ,\ v_{*j} = v'_{*j}\ ,$$
$$p_{*j} = P_j + p'_{*j}\ ,\ \eta_* = \overline{\eta}_* + \eta'_*. \tag{2.10}$$

Substitution into the basic equation with the neglect of higher order terms yields:

$$\frac{\partial u'_{*1}}{\partial t_*} + U_*\frac{\partial u'_{*1}}{\partial x_*} + v'_{*1}\frac{dU_*}{dy_*} = fv'_{*1} - \frac{1}{\rho}\frac{\partial p'_{*1}}{\partial x_*},$$
$$\frac{\partial u'_{*2}}{\partial t_*} = fv'_{*2} - \frac{1}{\rho}\frac{\partial p'_{*2}}{\partial x_*},$$
$$\frac{\partial v'_{*1}}{\partial t_*} + U_*\frac{\partial v'_{*1}}{\partial x_*} = -fu'_{*1} - \frac{1}{\rho}\frac{\partial p'_{*1}}{\partial y_*},$$
$$\frac{\partial v'_{*2}}{\partial t_*} = -fu'_{*2} - \frac{1}{\rho}\frac{\partial p'_{*2}}{\partial y_*},$$
$$p'_{*1} - p'_{*2} = \Delta\rho g\eta'_*,$$
$$\frac{\partial \eta'_*}{\partial t_*} = -U_*\frac{\partial \eta'_*}{\partial x_*} - \frac{\partial}{\partial x_*}\left(\overline{\eta}_* u'_{*1}\right) - \frac{\partial}{\partial y_*}\left(\overline{\eta}_* v'_{*1}\right),$$
$$= \frac{\partial}{\partial x_*}\left(\left(H - \overline{\eta}_*\right)u'_{*2}\right) + \frac{\partial}{\partial y_*}\left(\left(H - \overline{\eta}_*\right)v'_{*2}\right).$$

The variables x_* and y_* are non-dimensionalized by λ_R; u'_{*j}, v'_{*j} and U_* by $f\lambda_R$; t_* by $1/f$; $\overline{\eta}_*$ and η'_* by H; p_{*j} by $\Delta\rho gH$. Assuming a sinusoidal form in the x_*-direction $(u'_{*j}, v'_{*j}, p'_{*j}, \eta'_* \propto e^{ik(x-ct)})$, we get the non-dimensional equations:

$$-ikcu_1 + ikUu_1 + \frac{dU}{dy}v_1 = v_1 - ikp_1, \tag{2.11}$$
$$-ikcu_2 = v_2 - ikp_2, \tag{2.12}$$
$$-ikcv_1 + ikUv_1 = -u_1 - \frac{dp_1}{dy}, \tag{2.13}$$
$$-ikcv_2 = -u_2 - \frac{dp_2}{dy}, \tag{2.14}$$
$$p_1 - p_2 = \eta, \tag{2.15}$$
$$-ikc\eta = -ikU\eta - ik\overline{\eta}u_1 - \frac{d}{dy}(\overline{\eta}v_1), \tag{2.16}$$
$$= ik(1-\overline{\eta})u_2 + \frac{d}{dy}((1-\overline{\eta})v_2). \tag{2.17}$$

As in Section 2.2 in Iga (1993), the boundary conditions for non-dimensional variables are:

$$u_1, v_1 \quad \text{regular at } y = -Ri^{1/2}, \tag{2.18}$$
$$u_1 = -iv_1 \text{ at } y = 0, \tag{2.19}$$
$$u_2 = iv_2 \text{ at } y = -Ri^{1/2}, \tag{2.20}$$
$$u_2, v_2 \quad \text{regular at } y = 0. \tag{2.21}$$

2.3 Derivation of the eigenvalue problem

We will derive the equations of the form of $\mathsf{A}\boldsymbol{z} = c\boldsymbol{z}$ from equations (2.11) $\sim$ (2.17). Expressing the vorticity, divergence and the divergence of the mass transport in each layer, respectively, as:

$$\zeta_i \equiv ikv_i - \frac{du_i}{dy},$$
$$D_i \equiv iku_i + \frac{dv_i}{dy},$$
$$FD_1 \equiv ik\overline{\eta}u_1 + \frac{d}{dy}(\overline{\eta}v_1),$$
$$FD_2 \equiv ik(1-\overline{\eta})u_2 + \frac{d}{dy}((1-\overline{\eta})v_2),$$

(2.16) is rewritten as

$$-ikc\eta = -ikU\eta - FD_1. \tag{2.22}$$

Subtracting (2.22) from the vorticity equation in the lower layer

$$-ikc\zeta_1 = -ikU\zeta_1 - FD_1, \tag{2.23}$$

which is derived from $ik(2.13) - d/dy(2.11)$, we obtain the potential vorticity equation in the lower layer

$$-ikc(\zeta_1 - \eta) = -ikU(\zeta_1 - \eta). \tag{2.24}$$

On the other hand, using (2.15), the differences of the equation of motion between the two layers, (2.11)–(2.12) and (2.13)–(2.14) become

$$-ikc(u_1 - u_2) = -ikUu_1 + \overline{\eta}v_1 - v_2 - ik\eta, \tag{2.25}$$
$$-ikc(v_1 - v_2) = -ikUv_1 - u_1 + u_2 - \frac{d\eta}{dy}. \tag{2.26}$$

Since η is expressed as

$$ikU\eta = -FD_1 - FD_2, \tag{2.27}$$

which is derived from (2.16)–(2.17), we obtain the equations of the form of eigenvalue problem by substituting (2.27) into η in (2.24), (2.25), (2.26) and (2.17)

$$kc\left(\zeta_1 - \frac{iFD_1 + iFD_2}{kU}\right) = kU\left(\zeta_1 - \frac{iFD_1 + iFD_2}{kU}\right), \tag{2.28}$$
$$kc(u_1 - u_2) = kUu_1 + \overline{\eta}iv_1 - iv_2 + \frac{iFD_1 + iFD_2}{U}, \tag{2.29}$$
$$kc(iv_1 - iv_2) = kUiv_1 + u_1 - u_2 + \frac{d}{dy}\left(\frac{iFD_1 + iFD_2}{kU}\right), \tag{2.30}$$
$$kc(iFD_1 + iFD_2) = kUiFD_2. \tag{2.31}$$

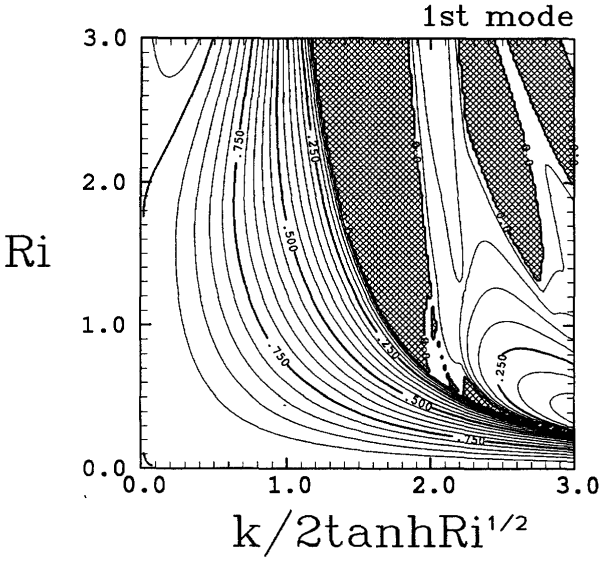

Fig. 6. The isolines of the imaginary part of phase speed of the fastest growing mode when the parameter Ri and wavenumber are given. We take $k/(2\tanh Ri^{1/2})$ as the wavenumber axis and showed the isolines of $2\sinh Ri^{1/2}\cdot c_i$ for convenience of comparison with the Fig. 3 in Iga (1993). The contour intervals are 0.05. Hatched areas indicate the regions where there is no unstable mode (where $|c_i|$ of the first mode is zero).

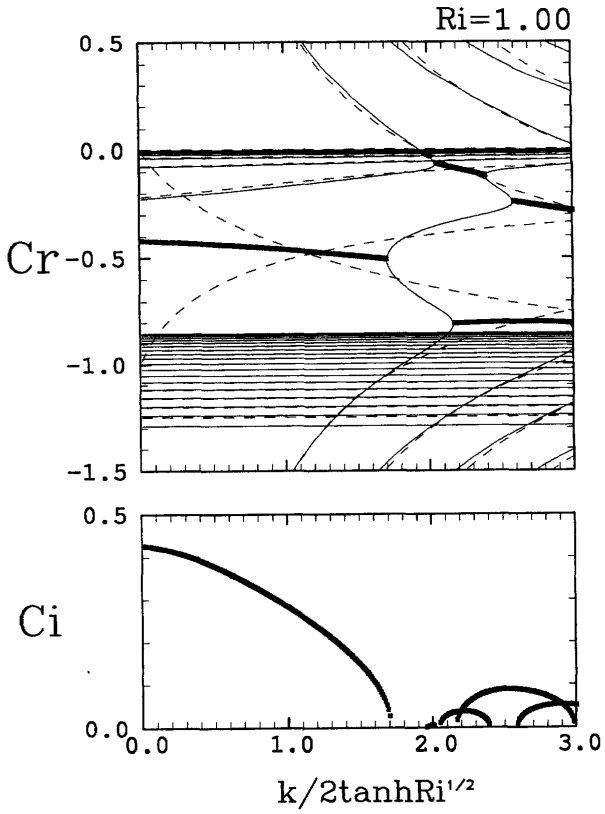

Fig. 7. The values of c_r and c_i as functions of $k/(2\tanh Ri^{1/2})$ at $Ri = 1.0$. Unstable modes are shown by thick lines. Dashed lines indicate the dispersion curves of the one-layer problems for the same Ri (see Section 4).

3. Numerical solutions

The eigenvalue problem of (2.28), (2.29), (2.30) and (2.31) was solved using finite differences. The numerical method in detail is described in the Appendix. Figure 6 shows the imaginary part of the phase speed of the fastest growing mode for each combination of parameter Ri and wavenumber k. For convenience of comparison with Fig. 3 in Iga (1993), we take $k/(2\tanh Ri^{1/2})$ instead of k as wavenumber axis, and displayed $2\sinh Ri^{1/2}\cdot c_i$ instead of c_i as the imaginary part of the phase speed. Dispersion relations in the cases of $Ri = 1.0$ and 3.0 are shown in Figs. 7 and 8.

As Fig. 6 shows, there are various unstable modes in this model; in particular, in the region of large Ri and k, some complicated unstable modes exist. From the dispersion relation for $Ri = 1.0$ shown in Fig. 7, we can see following features. There are families of unstable modes; all of them have phase speeds whose real parts are between about -1.0 and 0.0. Neutral waves are roughly classified into four groups: (i) modes with $c \sim 0.0$, (ii) modes with $c \sim -1.0$, (iii) modes whose phase speeds are positive and decrease as wavenumber increases, (iv) modes whose phase speeds are negative and approach 0 as wavenumber increases. The unstable modes appear where dispersion curves of these neutral modes intersect, but intersection of a mode in the group (ii) and a mode in (iv) does not cause unstable modes.[1] The fundamental features of dispersion relation for $Ri = 3.0$ are the same as those for $Ri = 1.0$, except that many higher modes appear.

4. Identification of unstable modes by resonances between neutral modes

We can obtain the modes in the two-layer frontal model by solving the eigenvalue problem in the previous section. Generally, unstable modes in two layer problems are clearly classified by comparing the dispersion curves in the whole two-layer problem and those in the reduced one-layer problems (see Sakai, 1989; Iga, 1993). Therefore, in this section, we will describe the reduced one-layer problems in each layer for the present case, and classify the obtained unstable modes.

1 We use here the term unstable mode as a mode whose eigenvalue has a positive imaginary part or a mode which grows exponentially. However, where two dispersion curves intersect and two eigenvalues are degenerate, may exist modes growing linearly, which are also commonly called unstable modes.

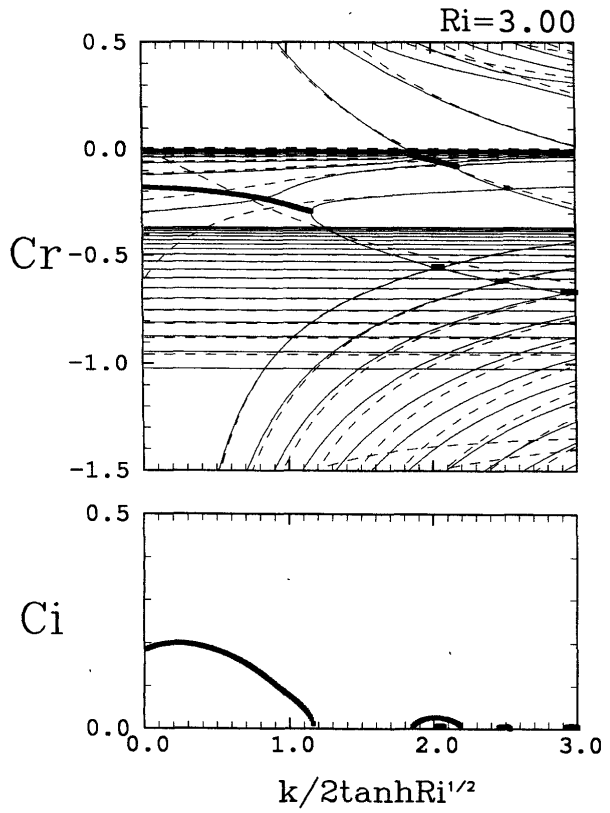

Fig. 8. Same as Fig. 7, but for $Ri = 3.0$.

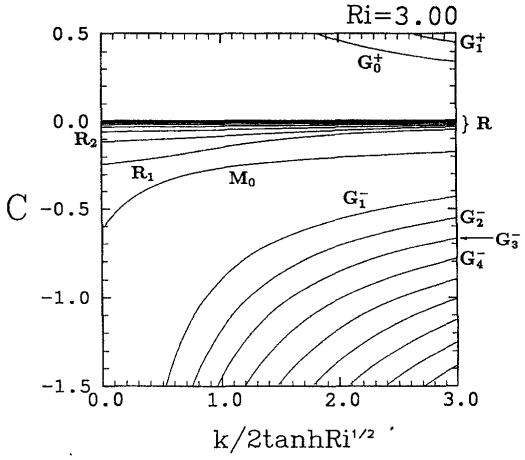

Fig. 9. Dispersion curves of neutral waves in the upper one-layer problem for $Ri = 3.0$. In this system exist Poincaré modes propagating in the positive (G_n^+) and negative (G_n^-) directions, Rossby modes whose phase propagates slowly in the negative direction (R_n), and a Kelvin mode whose feature changes with wavenumber (M_0).

First, we consider the one-layer problem for the upper layer. Since the fluid in the upper layer is at rest, the non-dimensionalized equations for each Fourier component are

$$-ikcu = v - ik\eta, \tag{4.1}$$

$$-ikcv = -u - \frac{d\eta}{dy}, \tag{4.2}$$

$$-ikc\eta = ik(1-\overline{\eta})u + \frac{d}{dy}((1-\overline{\eta})v). \tag{4.3}$$

The boundary conditions become

$$u = iv \text{ at } y = -Ri^{1/2}, \tag{4.4}$$

$$u, v \quad \text{regular at } y = 0. \tag{4.5}$$

For the lower layer, the equations are

$$-ikcu + ikUu + \frac{dU}{dy}v = v - ik\eta, \tag{4.6}$$

$$-ikcv + ikUv = -u - \frac{d\eta}{dy}, \tag{4.7}$$

$$-ikc\eta = -ikU\eta - ik\overline{\eta}u - \frac{d}{dy}(\overline{\eta}v), \tag{4.8}$$

and the boundary conditions are

$$u, v \quad \text{regular at } y = -Ri^{1/2}, \tag{4.9}$$

$$u = -iv \quad \text{at } y = 0. \tag{4.10}$$

We solved the eigenvalue problem of (4.1), (4.2) and (4.3) for the upper layer problem and the problem of (4.6), (4.7) and (4.8) for the lower layer problem also using finite differences. The results are shown in Figs. 9 and 10. In the one-layer problem for the upper layer, there exists a family of modes propagating in the positive direction (Fig. 9). These modes are Poincaré (gravity) modes, whose restoring force is basically the gravity force. We will call these modes $G_0^+, G_1^+, G_2^+, \cdots$ according to the number of nodes in y-direction. Gravity modes propagating in the negative direction $G_1^-, G_2^-, G_3^-, \cdots$ also exist in the same way. In addition, there exist modes whose phase propagates more slowly in the negative x-direction. These modes are Rossby modes; they are in geostrophic balance, and propagate based on the gradient of potential vorticity of the basic state. We call them $R_1, R_2, R_3, \cdots$ according to the number of nodes in the y-direction. Furthermore, a Kelvin mode M_0 exists which behaves like a Rossby wave when the wavenumber is small and becomes like a gravity wave as the wavenumber increases. These qualitative results are evident from the theory by Iga (1995).[2]

On the other hand, in the one-layer problem for the lower layer (Fig. 10), there are the family of modes $G_0^-, G_1^-, G_2^-, \cdots$, the family $G_1^+, G_2^+, G_3^+, \cdots$ and the mode M_0, just like the upper layer although

2 Note the discrepancies between the definition of modes by Iga (1995) and the name of modes in this paper. R-mode, G-mode and M-mode in this paper or in Iga (1993) are called Rossby mode, Poincaré mode and Kelvin mode in Iga (1995), respectively.

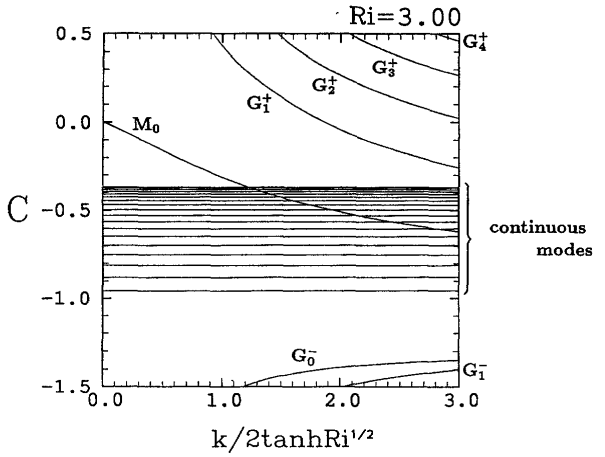

Fig. 10. Dispersion curves of neutral waves in the lower one-layer problem for $Ri = 3.0$. Poincaré (gravity) modes propagating in both directions ($G_n^{\pm}$) and M_0-mode exist, but Rossby modes (R_n) do not. Discretizations of continuous modes by finite differences appear instead.

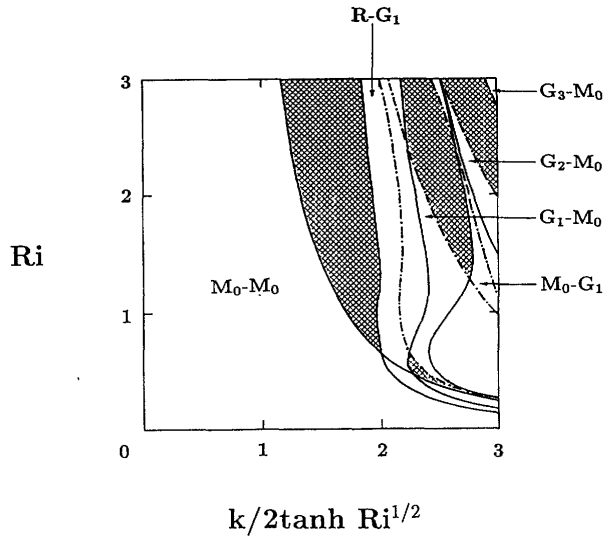

Fig. 11. The classification of the obtained unstable modes. R_1-M_0, for example, indicates that the unstable mode is caused by a resonance between the R_1-mode in the upper layer and the M_0-mode in the lower layer. There is no unstable mode in the cross-hatched regions.

the propagating directions are opposite. However, there is no Rossby mode in this system because of the uniformity of the potential vorticity of the basic state. Continuous modes caused by the shear of the basic state exist instead, and they appear as discretization by finite differences corresponding to each grid point.

The dashed lines in Figs. 7 and 8 show these dispersion curves in reduced one-layer problems. Comparing these dispersion curves with those in full two-layer problems, we can identify the modes in the two-layer problem: The modes in the group (i) are Rossby modes in the upper layer, the modes in the group (ii) are continuous modes appearing by finite differences, and the modes in the groups (iii) and (iv) correspond to Poincaré modes in each layer. Moreover, we can classify the unstable modes in the two-layer problem by the kinds of the resonating modes. The results are shown in Fig. 11.

5. Discussions

Let us compare the results in this model with those of earlier studies, mainly with those of Iga (1993) or of the frontal model with two homogeneous flows. First, comparing Figs. 6 and 11 with Figs. 3 and 11 in Iga (1993), the results are roughly alike in this parameter range; in particular, as to the M_0-M_0-mode, which occupies the major part in this region, the imaginary part of phase speed approaches the half of the difference of the velocities outside the frontal zone ($c_i \to 1$ in Iga (1993) since c_* is non-dimensionalized by $\Delta U/2$, and $c_i \to 1/(2\sinh Ri^{1/2})$ in this paper since c_* is non-dimensionalized by $f\lambda_R$) as either Ri or k decreases (in Iga (1993), the non-dimensionalized wavenumber is expressed as Ro), and as either Ri or k increases, $|c_i|$ diminishes its value finally to vanish.

Where Ri and k are large (the region of (H) in Orlanski (1968)), we can find corresponding modes such as R-G_1- or M_0-G_1-mode in both models and the results seem to be qualitatively the same, although there are some quantitative differences such as the shift of the regions where individual modes exist. Nevertheless, there is a mode which completely disappears in the model in this paper: R_1-R_1-mode and M_0-R_1-mode (called (E)-mode and (B)-mode in Orlanski (1968), respectively), which exist in the region of $Ri > 2$ and small k in the result by Iga (1993).

The differences of the unstable modes in the two models can be seen more clearly in the corresponding dispersion relations. Comparing Fig. 7 with Fig. 4 in Iga (1993) which show the dispersion relation in case of $Ri = 1.0$, we notice that the unstable modes with phase speeds close to the basic velocity of the upper layer ($c = 1$ for the result in Iga (1993) and $c = 0$ for the present model) behave in the same way. (The difference of phase speeds c is not essential, because it results from a difference in the coordinates system used.) However, the unstable modes with phase speeds close to the basic velocity of the lower layer ($c \sim -1.0$), are quite different. The unstable modes which exist in the frontal model with two layers of uniform velocity distribution, are stabilized in the model in this paper.

Therefore, although we mentioned earlier that we can find corresponding modes in the (H)-region in both models, this is only a superficial correspondence and some unstable modes disappear in the present model. In the frontal model of two homogeneous flows, unstable mode whose phase speed has non-zero real part (hatched in Fig. 11 in Iga (1993)) must be an overlapped pair of two modes, such as R-G_1- and G_1-R-modes, due to the symmetry of the situation. In the present model where the symmetry of the upper and lower layers is lost, the two unstable modes must appear separately. Numerical calculations, however, show the disappearance, for example, of the G_1-R-mode although the R-G_1-mode still exists.

We can understand this disappearance of unstable modes, with phase speeds close to the basic velocity of the lower layer, by the features of the waves in the reduced one-layer problems. First, as for the upper layer, there is no substantial difference between the models; qualitatively the same modes exist in both models, as expected by the theory by Iga (1995) and as demonstrated in the numerical results presented in this paper and Iga (1993). In contrast, there is a great difference between the two models in the lower layer. In the symmetrical model, the modes existing in the lower layer are completely the same as the upper layer. However, as for the model in this paper, there is no Rossby mode because of the uniformity of the potential vorticity in the basic state. The shear of the basic flow results in continuous modes instead.

The unstable modes with phase speeds close to the basic flow of the upper layer are mainly caused by resonance between a Rossby mode in the upper layer and a Poincaré mode in the lower layer. Since Rossby modes in the upper layer and Poincaré modes in the lower layer exist qualitatively in the same way in both models, the unstable modes caused by resonance between these modes appear in the same way in both models. On the other hand, the unstable modes with phase speeds close to the basic flow of the lower layer would arise from a resonance between a Poincaré mode in the upper layer and a Rossby mode in the lower layer. However, no Rossby mode exists in the lower layer in the present model and, as a result, the unstable modes do not exist. Continuous modes appear in this model instead of Rossby modes. They do not interact with the modes in the upper layer, since the equation (2.28) results in either

$$\zeta_1 - \frac{iFD_1 + iFD_2}{kU} = 0, \tag{5.1}$$

or

$$\zeta_1 - \frac{iFD_1 + iFD_2}{kU} = A\delta(y - y_c), \tag{5.2}$$

where $U(y_c) = c$,

and the problem is completely separated into equations which express continuous modes (5.2), (2.29), (2.30), (2.31) and those which express other non-singular modes (5.1), (2.29), (2.30), (2.31). In this way, the continuous modes in the lower layer which appear instead of Rossby modes do not interact with the modes in the upper layer in this model, and therefore the unstable modes with phase speeds close to the velocity of basic flow of the lower layer, which exist in the frontal model with two layers of uniform velocity distribution, are stabilized.

We can understand the absence of the R_1-R_1-mode ((E)-mode) for the same reason. On the other hand, we cannot explain the disappearance of the R_1-M_0-mode ((B)-mode) only by the absence of Rossby modes in the lower layer; the possibility of resonance between an R_1-mode in the upper layer and an M_0-mode in the lower layer still remains. From the dispersion curves in case of $Ri = 3.0$ (Fig. 8), it seems that the R_1-mode in the upper layer, though slightly modified, does not cause instability, since an unstable mode is already generated by two M_0-modes before the R_1-mode in the upper layer and the M_0-mode in the lower layer intersect, but the actual reason why R_1-M_0-mode disappears is still unclear.

Most of the other frontal models referred to in the introduction are essentially one-layer problems. Thus, there is no resonance between modes in the upper and lower layers. Moreover, the Rossby wave does not exist due to the uniformity of the potential vorticity. Therefore, there are no unstable modes in Paldor's (1983a) model, and there are only unstable modes caused by resonances between gravity waves (and Kelvin waves) in the same layer in the model of Paldor (1983b) or Kubokawa (1986), as pointed out by Sakai (1989). On the other hand, the model of Killworth *et al.* (1984) is also a two-layer problem with a layer of uniform potential vorticity, although it has a different configuration of frontal surface. We will compare the unstable modes obtained in the model in this paper also with the results in Killworth *et al.* (1984).

In the paper of Killworth *et al.* (1984), only the relation between wavenumber and growth rate (imaginary part of the phase speed) for a certain unstable mode is shown, but not the dispersion relation of neutral waves causing this unstable mode, which may be out of their interest. (Neither the dispersion relations for the reduced one-layer problems are shown, since the idea by Sakai (1989) that the unstable modes in a two-layer problem can be interpreted by the dispersion relations of one-layer problems was published later.) Hence, we cannot compare in detail the result in this paper with that of Killworth *et al.* (1984), but we can infer the features of the unstable modes in Killworth *et al.* (1984) to some extent, applying the theory by Iga (1995).

The unstable mode whose dispersion relation are shown in Killworth *et al.* (1984) exists between $k = 0$ to a certain finite wavenumber (Fig. 4 in their paper), and this is the same region as where the M_0-M_0-mode exist in this paper. Nevertheless, it is difficult to think that this mode shown by Killworth *et al.* (1984) can be the M_0-M_0-mode for the following reason. If we consider the reduced one-layer problems for the lower layer of this model, one of the boundary conditions is $H = 0$ and the M_0-mode is expected to exist in the same way as the model in this paper, but, for the upper layer, neither boundary is a closed boundary and no M_0-mode exists following the result by Iga (1995).[3] It is presumed that the mode shown in Killworth *et al.* (1984) is caused by resonance between the Kelvin mode in the lower layer and the first Rossby mode in the upper layer (R_1-M_0-mode). It is interesting that in a certain parameter range, both in the result by Iga (1993) and that in the model of Killworth *et al.* (1984), the R_1-M_0-mode with a node inside grows fastest, for which energy conversion into the disturbance occurs locally, while in the intermediate situation of this paper, the M_0-M_0-mode without a node is the fastest growing mode, for which energy conversion occurs throughout the disturbance.

6. Conclusions

We investigated the unstable modes in a frontal model whose lower layer has a uniform potential vorticity. We compared the results with those of other models, in particular with those of Iga (1993) which treats the front with two uniform flows formulated by Kotschin (1932). As a result, unstable modes with phase speeds close to the velocity of the basic flow in the lower layer which exist in the model in Iga (1993), are stabilized in the model in this paper. This is the result of the absence of a Rossby mode in the lower layer owing to the uniformity of the potential vorticity. Continuous modes which exist instead, do not interact with the modes in the upper layer. In addition, we compare the results with those obtained by Killworth *et al.* (1984), and find that the most dominant growing mode in that model is different from that in this model.

In such situations, we can understand the unstable modes by resonance between neutral modes in the both layers, and the modes which exist in each layer, in particular Rossby modes, are definitely affected the distribution of potential vorticity gradient. Therefore, whether a simplified model like Kotschin's (1932) has qualitatively the same features as more complicated situations depends on whether the potential vorticity gradient is similar.

The model with uniform potential vorticity is worth investigating as a fundamental model where certain modes are excluded. It is a model describing the critical situation which is interesting in the context of geophysical fluid dynamics. On the other hand, the result obtained in the model with two uniform flows, which seems a very special situation at a glance, is not at all special concerning the potential vorticity distribution. The obtained result can be extensively applied to other situations, for example, situations between the two cases: the case wherein the potential vorticity is uniform and that wherein the velocity is uniform.

The situation of almost uniform potential vorticity distribution like the front in the convergent cloud band over the Japan Sea, is so close to this critical situation that we must notice that situations which seem to be similar may have completely different stability. For the present, it is difficult to judge which model is more appropriate to apply to such real fronts, since, unfortunately, there is no dense observation of the fronts and meso-scale lows over the Japan Sea, although there are studies which compared a simple model with observation of real fronts as for similar fronts in other regions (Paldor *et al.* 1994). Data of potential vorticity distribution of the front as well as the structure of the developed disturbances would be an important key-point for applying a simple theory and understanding the mechanism of this phenomenon.

Acknowledgments

The author thanks Professor R. Kimura for motivating this problem and his encouragement throughout this study. He also would like to express thanks to Dr. K. Tsuboki for providing the data of numerical simulation of Japan Spectral Model (JSM). He also expresses thanks to the staff members of the Numerical Prediction Division, Japan Meteorological Agency, who originally developed this model. He is grateful to Professor G.W.K. Moore for reading the manuscript and making valuable comments. The LAPACK Library was used to solve the eigenvalue problem and the NCARG Library to draw some figures.

Appendix

A. Numerical calculations by finite differences

ζ_j, D_j, and FD_j are calculated from u_j and v_j as follows ($\Delta y \equiv Ri^{1/2}/N$):

$$\zeta_{j(l-\frac{1}{2})} = ikv_{j(l-\frac{1}{2})} - \frac{1}{\Delta y}\left(u_{j(l)} - u_{j(l-1)}\right), \quad \text{(A.1)}$$

$$D_{j(l)} = \frac{1}{\Delta y}\left(v_{j(l+\frac{1}{2})} - v_{j(l-\frac{1}{2})}\right) + iku_{j(l)}, \quad \text{(A.2)}$$

3 Strictly speaking, this situation is beyond the discussion in Iga (1995). In this problem the region extends to infinity, but both H and f remain finite. However, from the analogy of the result by Huthnance (1975), we can infer that this boundary condition behaves in the same way as neutral boundary conditions except for the existence of Poincaré continuum.

$$FD_{j(l)} = \frac{1}{\Delta y}\left(\overline{\eta}_{j(l+\frac{1}{2})}v_{j(l+\frac{1}{2})} - \overline{\eta}_{j(l-\frac{1}{2})}v_{j(l-\frac{1}{2})}\right) + ik\overline{\eta}_{j(l)}u_{j(l)}, \tag{A.3}$$

where $\overline{\eta}_2$ and U are defined by

$$U_{(l+\frac{1}{2})} = \frac{1}{2}\left(U_{(l)} + U_{(l+1)}\right),$$
$$U_{(l+\frac{1}{2})} = \frac{1}{\Delta y}\left(\overline{\eta}_{2(l+1)} - \overline{\eta}_{2(l)}\right),$$
$$\overline{\eta}_{2(l+\frac{1}{2})} = \frac{1}{2}\left(\overline{\eta}_{2(l)} + \overline{\eta}_{2(l+1)}\right),$$
$$\overline{\eta}_{2(l+\frac{1}{2})} = \frac{1}{\Delta y}\left(U_{(l+1)} - U_{(l)}\right),$$
$$\overline{\eta}_{2(0)} = 1, \quad \overline{\eta}_{2(N)} = 0,$$

and $\overline{\eta}_1$ is calculated as

$$\overline{\eta}_{1(l)} \equiv 1 - \overline{\eta}_{2(l)}.$$

Using these variables, (2.28)~(2.31) are finite differenced as follows

$$kc\left[\zeta_{1(l-\frac{1}{2})} - \frac{1}{2}\left(\frac{iFD_{1(l-1)} + iFD_{2(l-1)}}{kU_{(l-1)}} + \frac{iFD_{1(l)} + iFD_{2(l)}}{kU_{(l)}}\right)\right] = kU_{(l-\frac{1}{2})}\left[\zeta_{1(l-\frac{1}{2})} - \frac{1}{2}\left(\frac{iFD_{1(l-1)} + iFD_{2(l-1)}}{kU_{(l-1)}} + \frac{iFD_{1(l)} + iFD_{2(l)}}{kU_{(l)}}\right)\right], \tag{A.4}$$

$$kc\left(u_{1(l)} - u_{2(l)}\right) = kU_{(l)}u_{1(l)} + \frac{1}{2}\left(\overline{\eta}_{1(l-\frac{1}{2})}iv_{1(l-\frac{1}{2})} + \overline{\eta}_{1(l+\frac{1}{2})}iv_{1(l+\frac{1}{2})}\right) - \frac{1}{2}\left(iv_{2(l-\frac{1}{2})} + iv_{2(l+\frac{1}{2})}\right) + \frac{iFD_{1(l)} + iFD_{2(l)}}{U_{(l)}}, \tag{A.5}$$

$$kc\left(iv_{1(l-\frac{1}{2})} - iv_{2(l-\frac{1}{2})}\right) = kU_{(l-\frac{1}{2})}iv_{1(l-\frac{1}{2})} + \frac{1}{2}\left(u_{1(l-1)} + u_{1(l)}\right) - \frac{1}{2}\left(u_{2(l-1)} + u_{2(l)}\right) + \frac{1}{\Delta y}\left(\frac{iFD_{1(l)} + iFD_{2(l)}}{kU_{(l)}} - \frac{iFD_{1(l-1)} + iFD_{2(l-1)}}{kU_{(l-1)}}\right), \tag{A.6}$$

$$kc\left(iFD_{1(l)} + iFD_{2(l)}\right) = kU_{(l)}iFD_{2(l)}. \tag{A.7}$$

Computations in Section 3 were done with $N = 20$. The results were tested with $N = 40$ at some parameters. There was no qualitative difference between results with $N = 20$ and those with $N = 40$. Furthermore, some unstable modes were recomputed by the shooting method with many more grid points ($N = 20000$). As we can see from Fig. 12, the basic feature of the eigenfunction does not change, although the eigenvalue shifts a little. Thus, the relatively coarse resolution does not affect the discussions on the features of the unstable modes.

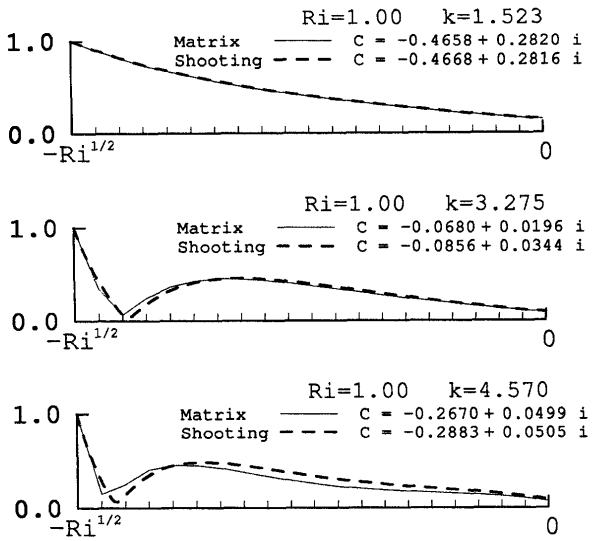

Fig. 12. The amplitude $|u_1|$ solved by matrix method with $N = 20$ and shooting method with $N = 20000$, normalized by the value of $|u_1|$ at $y = -\sqrt{Ri}$. The results solved by matrix method are shown by solid lines, and those by the shooting method by thick dashed lines. The panels show the fastest-growing mode for $Ri = 1.0$, $k = 1.523(= 2.0 \times \tanh 1.0)$, $Ri = 1.0$, $k = 3.275(= 4.3 \times \tanh 1.0)$ and $Ri = 1.0$, $k = 4.570(= 6.0 \times \tanh 1.0)$, and they are classified as the M_0-M_0-mode, R-G_1-mode and M_0-G_1-mode, respectively.

References

Huthnance, J.M., 1975: On trapped waves over a continental shelf. *J. Fluid Mech.*, **69**, 689–704.

Iga, K., 1993: Reconsideration of Orlanski's instability theory of frontal waves. *J. Fluid Mech.*, **255**, 213–236.

Iga, K., 1995: Transition modes of rotating shallow water waves in a channel. *J. Fluid Mech.*, **294**, 367–390.

Killworth, P.D., N. Paldor and M.E. Stern, 1984: Wave propagation and growth on a surface front in a two-layer geostrophic current. *J. Mar. Res.*, **42**, 761–785.

Kotschin, N., 1932: Über die Stabilität von Margulesschen Diskontinuitätsflächen. *Beitr. Phys. Atmos.*, **18**, 129–164.

Kubokawa, A., 1986: Instability caused by the coalescence of two modes of a one-layer frontal model. *J. Oceanogr. Soc. Japan*, **42**, 373–380.

Moore, G.W.K. and W.R. Peltier, 1990: Nonseparable baroclinic instability. part II: primitive-equations dynamics. *J. Atmos. Sci.*, **47**, 1223–1242.

Nagata, M. 1987: On the structure of a convergent cloud band over the Japan Sea; a prediction experiment. *J. Meteor. Soc. Japan*, **65**, 871–883.

Orlanski, I., 1968: Instability of frontal waves. *J. Atmos. Sci.*, **25**, 178–200.

Paldor, N., 1983a: Linear stability and stable modes of geostrophic modes. *Geophys. Astrophys. Fluid Dyn.*, **24**, 299–326.

Paldor, N., 1983b: Stability and stable modes of coastal fronts. *Geophys. Astrophys. Fluid Dyn.*, **27**, 217–228.

Paldor, N., C.-H. Liu, M. Ghil and R.M. Wakimoto, 1994: A new frontal instability: theory and ERICA observations. *J. Atmos. Sci.*, **51**, 3227–3237.

Sakai, S., 1989: Rossby-Kelvin instability: a new type of ageostrophic instability caused by a resonance between Rossby waves and gravity waves. *J. Fluid Mech.*, **202**, 149–176.

Snyder, C. 1995: Stability of steady fronts with uniform potential vorticity. *J. Atmos. Sci.*, **52**, 724–736.

Yamaguchi, K. and C. Magono, 1974: On the vortical disturbances in small scale accompanied with the meso scale front in Japan Sea in winter season. *Tenki*, **21**, 83–88. (in Japanese)

一層の渦位が一様である前線の不安定性

伊賀啓太

（東京大学海洋研究所）

2層のうちの下方の層の渦位が一様であるような前線の線形安定性について調べた。得られた結果を、両層ともに一様流からなる前線の不安定モードと比較した。両層ともに一様流である前線モデルにおいて存在した不安定モードのうち、下層の流速に近い位相速度を持つ不安定モードは、このモデルでは安定化していることがわかった。このことは下層1層だけの問題を考えた時に、渦位の一様性のためロスビー波が存在しないことで説明できる。前線の安定性には渦位分布が強く影響を与え、渦位が一様であるという臨界的な状況の前線モデルを適用する際には十分な注意が必要である。